

Topological phase transitions and topological Mott insulator in Haldane-Hubbard model

Zhao-Long Gu, Kai Li, and Jian-Xin Li

*National Laboratory of Solid State Microstructures & Department of Physics,
Nanjing University, Nanjing, 210093, China and*

Collaborative Innovation Center of Advanced Microstructures, Nanjing University, Nanjing 210093, China
(Dated: March 25, 2022)

Topological phase transitions and the phase diagram of Haldane-Hubbard model are investigated using the variational cluster approach. With increasing the interaction strength, there are two successive topological phase transitions. The first is characterized by the closing and reopening of the single particle gap with the Chern number changing its sign, while the second is featured by the divergence of the topological Hamiltonian's spectrum with the Chern number changing from a non-zero integer to zero. The second topological phase transition is not accompanied with the single particle gap closing but is associated with the zeros of the single particle Green's function. Between these two topological phase transitions, there exists a non-magnetic topological Mott insulating phase with no gapless single particle edge states which cannot be adiabatically connected to any non-interacting Chern insulator.

Nontrivial band topology has become one of the central interests in modern condensed matter physics since the discovery of topological insulator[1, 2]. Strong correlations, which results in many exotic phenomena, such as the fractional quantum Hall effect[3] and high temperature superconductivity[4], on the other hand, has been a major topic of the community in the past several decades. The interplay of these two ingredients leads to more richer physics[5–13], and meanwhile, leaves many important questions that are not fully answered, specifically, what is the fate of the nontrivial band topology when the system turns on strong electron-electron interactions, does it survive the Mott transition or will it just be destroyed by the correlations, and if there are topological phase transitions, how can one characterize it.

Previous works on the time reversal invariant Kane-Mele-Hubbard model shows that the Z_2 topology[14] are destroyed by the Hubbard interaction, accompanying with the closing and reopening of the single particle gap in the bulk and the absence of gapless single particle states on the edge[8, 15]. Whereas another model, the Haldane-Hubbard model[16–18], which breaks time reversal symmetry, is likely to host nontrivial strongly correlated phases. The mean field theory shows that when the original topological gap is small, there is a narrow window where both a non-zero Chern number and the antiferromagnetic (AF) order with a small moment exist[16–18]. With further increasing the interaction strength, the single particle gap closes and the system undergoes a topological phase transition as a result of the competition between the AF order and the original topological gap. When the original topological gap is large, the non-trivial topology may be directly destroyed by a first-order transition to a canted magnetic ordered phase without closing but leaving a discontinuous jump of the single particle gap[17]. More sophisticated slave-particle mean-field theories show that a gapped chiral

spin liquid phase or a Z_2 -double-semion-typed phase may exist when the interaction strength takes intermediate values[19–21]. Experimentally, the Haldane model has been realized recently in cold-atom experiments using the shaking lattice technique[22].

In this letter, using the variational cluster approach (VCA)[23], we show that the nontrivial band topology does survive the Mott transition in Haldane-Hubbard model when the original topological gap is small but finite. However, different from previous works, we find that the on-site Hubbard interaction drives the system to undergo two successive topological phase transitions rather than only one. The first is identified as the Mott transition that the original topological band gap closes and a new one reopens, accompanying with the change of the sign of the system's Chern number, and the second occurs when the AF order is large enough to turn the Chern number to zero without the closure of the single particle gap but with a divergence of the topological Hamiltonian's spectrum. Remarkably, this divergence coincides with the appearance of the zeros of the single particle Green's function. It turns out to be a realization in a microscopic model that the zeros of the single particle Green's function marks the topological phase transition[24]. Moreover, the AF order actually does not form immediately after the Mott transition, leaving a non-magnetic phase with a non-zero Chern number. We thus identify this phase as a topological Mott insulator (TMI). However, different from that proposed by S. Raghu et. al.[25], this phase has no gapless single particle edge states so that it cannot be adiabatically connected to any non-interacting band insulators with non-zero Chern numbers. This fact indicates that we find a new topological state of matter due to the presence of the correlations between electrons. Finally, similar to the mean field results, with the further increase of the interaction strength after the Mott transition, the AF order

sets in and coexists with non-trivial topology for a narrow window of parameters before the second topological phase transition occurs.

The Haldane-Hubbard model is defined as $H = H_0 + H_U$, where H_0 is the model proposed by Haldane[26] on the honeycomb lattice as shown in Fig. 1(a),

$$H_0 = -t \sum_{\langle ij \rangle \sigma} c_{i\sigma}^\dagger c_{j\sigma} - it' \sum_{\langle\langle ij \rangle\rangle \sigma} \nu_{ij} c_{i\sigma}^\dagger c_{j\sigma} - \mu \sum_{i\sigma} c_{i\sigma}^\dagger c_{i\sigma} \quad (1)$$

and H_U is the Hubbard interaction,

$$H_U = U \sum_i n_{i\uparrow} n_{i\downarrow} \quad (2)$$

Here, $\langle ij \rangle$ and $\langle\langle ij \rangle\rangle$ denote the nearest neighbor (NN) and the next nearest neighbour (NNN) bonds, respectively. $\nu_{ij} = +1(-1)$ if the electron makes a left (right) turn to get to the NNN site. μ is the chemical potential and is so chosen as to make the system at half filling. Others are in standard notation. Throughout this letter, we use t as the energy unit. Due to the pure imaginary NNN hopping it' , this model breaks the time reversal symmetry locally and there exists non-homogeneous flux in the honeycomb lattice but the total flux through every single hexagon is zero. As a consequence, in the non-interacting limit, the ground state of the system has a non-zero Chern number and is a quantum anomalous Hall insulator (QAHI) or a Chern insulator (CI).

VCA[23] is the variational version of cluster perturbation theory (CPT)[27] while the latter is a quantum cluster approach to calculate the single particle Green's functions for interacting many-body systems. In CPT, the lattice is tiled into superlattice of clusters. The decoupled clusters are solved exactly and the inter-cluster single particle terms are treated as perturbations. The thermodynamic single particle Green's function $G(\omega, \mathbf{k})$ of the system is then obtained through an RPA-like equation:

$$G^{-1}(\omega, \mathbf{k}) = G_0^{-1}(\omega) - V(\mathbf{k}) \quad (3)$$

where $G_0(\omega)$ and $V(k)$ represent the exact cluster Green's function and the inter-cluster single particle terms, respectively. CPT has the advantages that it treats local spatial quantum fluctuations exactly in small clusters and it can get the full momentum distribution of the spectral function after the periodization[28]. However, due to the finite size effect, CPT alone cannot find spontaneous symmetry breaking phases. Based on the self-energy functional theory[29], VCA on the other hand, is able to touch such phases, by taking the decoupled clusters as the reference system and varying the grand potential with respect to added Weiss fields. A symmetry-breaking phase in VCA is reached if the grand potential takes its minimum at a finite value of the corresponding Weiss field.

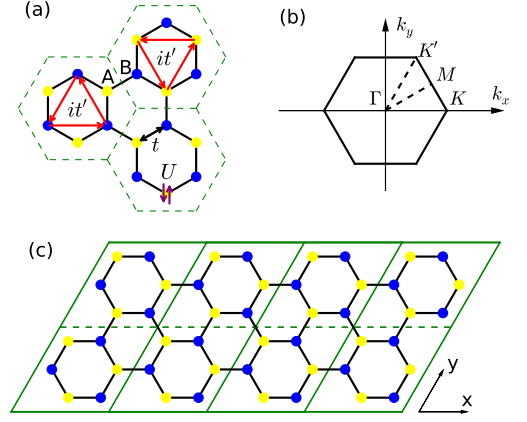


FIG. 1. (color online). (a) 6-site cluster tiling (the hexagon enclosed by the green dashed lines) on honeycomb lattice used for the calculations of bulk properties. A and B denote the two inequivalent sites. The hopping amplitudes t , it' and the Hubbard interaction U of Haldane-Hubbard model are also shown. (b) The first Brillouin zone (FBZ). (c) An illustration of tiling the armchair ribbon used for the calculations of edge states. The superlattices (parallelogram with green solid lines) are arranged periodically along the x direction. For illustration, we only plot two clusters (separated by the green dashed line) in each superlattice, while in the calculations fifteen clusters are included.

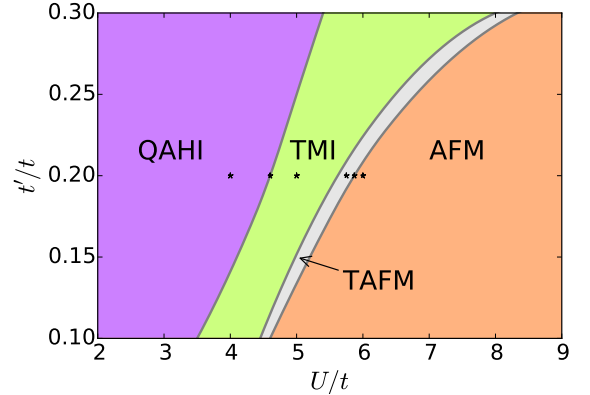


FIG. 2. (color online). Phase diagram of the Haldane-Hubbard model. QAHI, TMI, TAFM and AFM denote quantum anomalous Hall insulator, topological Mott insulator, topological antiferromagnetic Mott insulator and antiferromagnetic Mott insulator, respectively. Stars mark the points at which $\Delta\Omega$ is plotted in Fig. 3(a) and the spectrum is plotted in Fig. 4.

In interacting many-body systems, the single particle Green's function is a useful tool to investigate the topological properties[30–32]. Recently, it has been proved that the zero-frequency single particle Green's function alone is sufficient to encode all the topological information if the system has no non-trivial ground state degeneracies[33]. Then the so-called topological

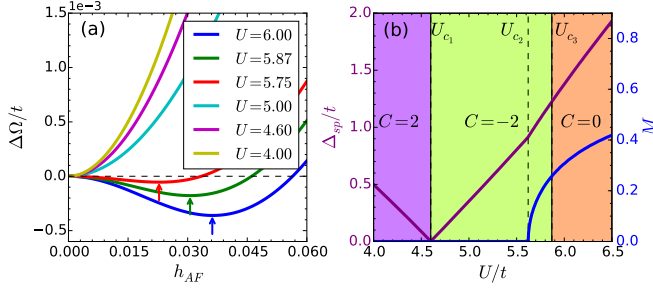


FIG. 3. (color online). (a) $\Delta\Omega$ as a function of h_{AF} for $t' = 0.2$. Arrows indicate the positions of the minima, where magnetic solutions are allowed. (b) The Chern number C , the single particle gap Δ_{sp} and the antiferromagnetic order M as a function of U for $t' = 0.2$. $U_{c1} = 4.60$, $U_{c2} = 5.62$ and $U_{c3} = 5.87$ represent the first topological transition point, the paramagnetic antiferromagnetic transition point and the second topological transition point, respectively.

Hamiltonian[34], which is defined as,

$$H_{topo}(\mathbf{k}) = -G^{-1}(\omega, \mathbf{k})|_{\omega=0} \quad (4)$$

can be used to compute topological invariants. In this letter, we use this quantity to calculate the Chern numbers.

The phase diagram of Haldane-Hubbard model is shown in Fig. 2. We use the Chern number C , the single particle gap Δ_{sp} , and the AF moment M as the order parameters to determine the phases and their boundaries. These order parameters are calculated using VCA on the 6-site-cluster-tiled superlattice as illustrated in Fig. 1(a). This cluster not only preserves the point-group symmetry of the Hamiltonian but also has zero net flux through it, which makes it the best choice in the calculations. There are four distinct phases separated by three phase boundaries. The Chern number is 2 for QAH, -2 for TMI and TAFM, and 0 for AFM. The single particle gap keeps non-zero except on the transition line from QAH to TMI. The AF moment is non-zero for TAFM and AFM.

Take $t' = 0.2$ as an example, let's have a close look at these order parameters. Δ_{sp} and M are computed at the minimum points of the grand potential Ω with respect to the AF Weiss field: $H_{AF} = h_{AF} \sum_i (-1)^{\eta_i} c_{i\alpha}^\dagger \sigma_{\alpha\beta}^z c_{i\beta}$ where $\eta_i = 0$ or 1 when $i \in A$ or B . In Fig. 3(a), $\Delta\Omega = \Omega(h_{AF}) - \Omega(h_{AF} = 0)$ at the stated points in Fig. 2 are shown. It is clear that for small Hubbard interactions, $\Delta\Omega$ s take their minima when $h_{AF} = 0$, indicating the system is in the paramagnetic state while for large Hubbard interactions $\Delta\Omega$ s reach their minima when h_{AF} is non-zero, meaning the AF moment has already formed. In Fig. 3(b), C , Δ_{sp} and M are plotted for a range of Hubbard interactions. With increasing U , it can be seen that Δ_{sp} decreases linearly at first, gets to zero at U_{c1} , then increases linearly with a different absolute value of the slope, and then encounters a second

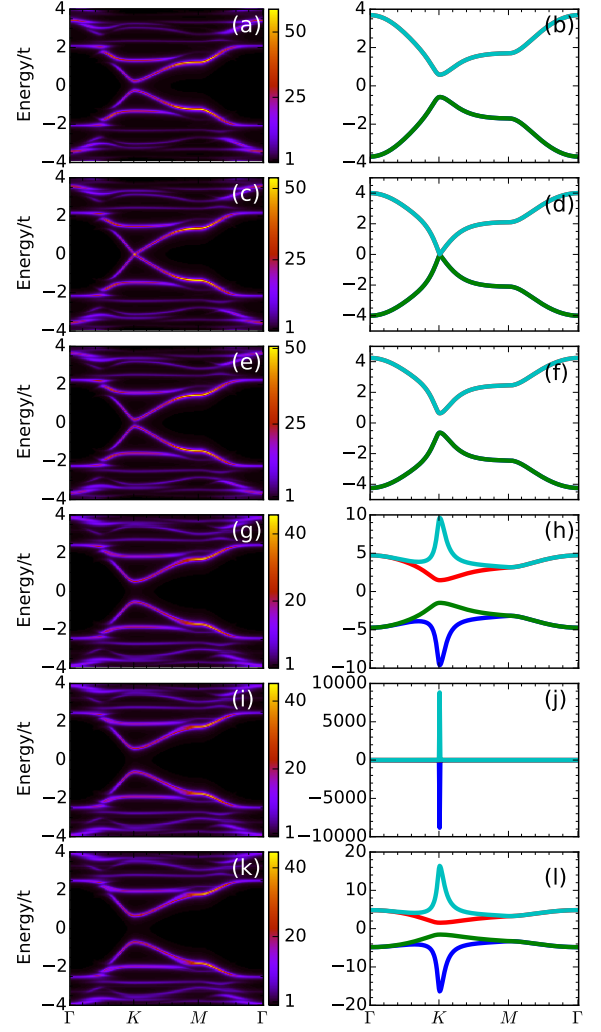


FIG. 4. (color online). Single particle spectra and the topological Hamiltonian's spectra along the high symmetry path in the FBZ calculated with (a)-(b) $U = 4.00$, $h_{AF} = 0$, (c)-(d) $U = 4.60$, $h_{AF} = 0$, (e)-(f) $U = 5.00$, $h_{AF} = 0$, (g)-(h) $U = 5.75$, $h_{AF} = 0.0228$, (i)-(j) $U = 5.87$, $h_{AF} = 0.0306$, and (k)-(l) $U = 6.0$, $h_{AF} = 0.0362$. The values of h_{AF} are determined by the locations of $\Delta\Omega$ s' minima in Fig. 3(a). The NNN hopping is fixed at $t' = 0.2$.

change of the slope at U_{c2} where the AF moment M develops a non-zero value continuously. The Chern number changes its sign at U_{c1} but does not change immediately after the AF order appears. On the contrary, the non-trivial topology coexists with the AF order for a small window of U . More exotically, there isn't any singularity of Δ_{sp} and M at U_{c3} where the Chern number changes from -2 to 0.

It is well believed that in the non-interacting limit, topological phase transitions cannot occur without closing the single particle gap. In fact, this is also applied to the interacting regime when the interaction is not strong enough to induce an AF order, as what hap-

pens at the first topological phase transition as discussed above. However, the second topological phase transition is quite different: it is not accompanied by the single particle gap closing. To investigate the features of these two topological phase transitions, in Fig. 4, we plot the single particle spectra and the topological Hamiltonian's spectra at the stated points indicated in Fig. 2. With increasing the Hubbard interaction strength U , before the AF moment forms, the single particle spectra and the topological Hamiltonian's spectra show similar evolution behavior: their gaps both close at the first topological transition point. However, after the formation of the AF moment, their behavior deviates from each other essentially. The single particle spectra exhibit few changes except that the gap increases linearly while the topological Hamiltonian's spectra quickly develop a divergence toward the second topological phase transition point.

In general, the single particle self energy $\Sigma(\omega, \mathbf{k})$ can be decomposed as $\Sigma(\omega, \mathbf{k}) = \Sigma_1(\mathbf{k}) + \Sigma_2(\omega, \mathbf{k})$, where $\Sigma_1(\mathbf{k})$ is the static part that only renormalizes the band structure, and $\Sigma_2(\omega, \mathbf{k})$ is the dynamical part that comes from quantum fluctuations. From Eq. 4, it is clear that the topological Hamiltonian's spectrum coincides with the single particle spectrum when only Hartree-Fock diagrams are taken into considerations since they only contribute to $\Sigma_1(\mathbf{k})$. However, in a general case, the former does not represent any quasi-particle spectrum because of the Σ 's dependency on ω . In Haldane-Hubbard model, as is previously discussed, we can conclude that the dynamical part $\Sigma_2(\omega, \mathbf{k})$ varies considerably with respect to ω around the second topological phase transition point and diverges at zero frequency at this point. This divergence means the existence of a zero eigenvalue of the single particle Green's function and is another kind of singularity other than poles. This singularity lies in the Mott gap where the single particle spectral function is already zero, so we cannot easily extract its information from the single particle spectrum. The second topological phase transition is driven by dynamical effects which goes beyond the mean field pictures and is associated with the zeros of the single particle Green's function.

Between these two topological phase transitions, there exists a non-magnetic TMI. This phase respects all the symmetries of the Hamiltonian and its Chern number is opposite to that of the QAHI it transited from. In the non-interacting limit, we can construct another QAHI by merely reversing the sign of the NNN hopping it' and at first sight this constructed phase has the same properties with the fore-mentioned TMI: they have equal Chern numbers. However, these Chern numbers may have different physical meanings because in the presence of strong interactions the Chern number does not necessarily represent the Hall conductivity. To clarify whether these two phases are identical to each other, in Fig. 5, we plot the single particle spectra calculated by VCA on an armchair ribbon as is illustrated in Fig. 1(c). In order

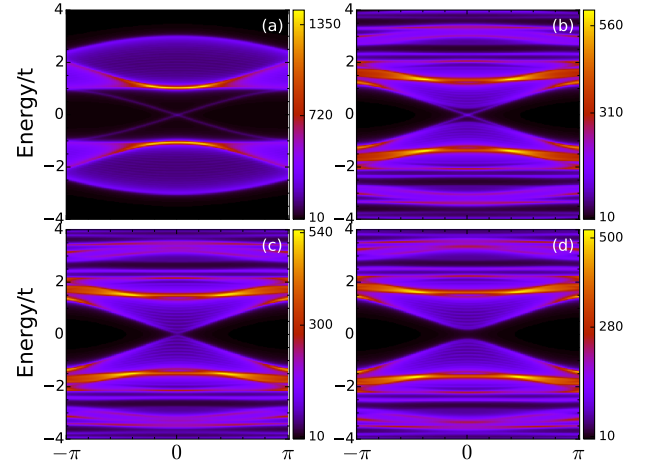


FIG. 5. (color online). Intensity plot of the single particle spectra calculated on the armchair ribbon illustrated in Fig. 1(c) with (a) $U = 0$, (b) $U = 4.00$, (c) $U = 4.60$, and (d) $U = 5.00$. The NNN hopping is fixed at $t' = 0.2$.

to completely tiling the strip, a 6-site cluster is used. In realistic calculations, fifteen clusters are included in the y direction to form a supercluster and the superclusters are arranged periodically in the x direction. For illustration, we only show schematically two superclusters in the y direction in Fig. 1(c). It can be seen that the gapless single particle edge states disappear after the bulk state has transited to the TMI. However, according to the bulk-edge correspondence, any non-interacting system with non-zero Chern numbers should have gapless single particle edge states. This fact indicates that the TMI reported here cannot be adiabatically connected to any non-interacting Chern insulator, so it has no free counterparts. Our numerical method cannot give more properties of this phase but it is desirable to consider the possibility of the fractionalized Chern insulator proposed by slave-particle mean field theories[19–21]. However, it's still an open question to ask whether or not the electrons are fractionalized in this phase.

In summary, we have shown that there are two successive topological phase transitions with different features in the Haldane-Hubbard model with increasing the Hubbard interaction strength, of which the first is characterized by the usual single particle gap closing while the second is associated with the zeros of the single particle Green's function and is driven by dynamical effects. Between these two topological phase transitions there exists a non-magnetic topological Mott insulator with no gapless single particle edge states.

Note added. We find a related work done by Wu *et al.* Ref.[35] after the completion of the writing of this paper.

We acknowledge helpful discussions with Shun-Li Yu, Zhong Wang, Jin-Guo Liu and Wei Wang. This work was supported by the National Natural Science Foundation of China (11190023 and 11374138).

-
- [1] X.-L. Qi and S.-C. Zhang, *Rev. Mod. Phys.* **83**, 1057 (2011).
 - [2] M. Z. Hasan and C. L. Kane, *Rev. Mod. Phys.* **82**, 3045 (2010).
 - [3] H. L. Stormer, D. C. Tsui, and A. C. Gossard, *Rev. Mod. Phys.* **71**, S298 (1999).
 - [4] P. A. Lee, N. Nagaosa, and X.-G. Wen, *Rev. Mod. Phys.* **78**, 17 (2006).
 - [5] G. Jackeli and G. Khaliullin, *Phys. Rev. Lett.* **102**, 017205 (2009).
 - [6] D. Pesin and L. Balents, *Nature Physics* **6**, 376 (2010).
 - [7] M. Hohenadler, T. C. Lang, and F. F. Assaad, *Phys. Rev. Lett.* **106**, 100403 (2011).
 - [8] S.-L. Yu, X. C. Xie, and J.-X. Li, *Phys. Rev. Lett.* **107**, 010401 (2011).
 - [9] N. Regnault and B. A. Bernevig, *Phys. Rev. X* **1**, 021014 (2011).
 - [10] C. Griset and C. Xu, *Phys. Rev. B* **85**, 045123 (2012).
 - [11] W. Wu, S. Rachel, W.-M. Liu, and K. Le Hur, *Phys. Rev. B* **85**, 205102 (2012).
 - [12] J. Maciejko and G. A. Fiete, *Nature Physics* **11**, 385 (2015).
 - [13] Q.-X. Li, R.-Q. He, and Z.-Y. Lu, *Phys. Rev. B* **92**, 155127 (2015).
 - [14] C. L. Kane and E. J. Mele, *Phys. Rev. Lett.* **95**, 146802 (2005).
 - [15] F. Grandi, F. Manghi, O. Corradini, C. M. Bertoni, and A. Bonini, *New Journal of Physics* **17**, 023004 (2015).
 - [16] J. He, Y.-H. Zong, S.-P. Kou, Y. Liang, and S. Feng, *Phys. Rev. B* **84**, 035127 (2011).
 - [17] W. Zheng, H. Shen, Z. Wang, and H. Zhai, *Phys. Rev. B* **91**, 161107 (2015).
 - [18] V. Arun, R. Sohal, C. Hickey, and A. Paramekanti, *arXiv:1510.08856* (2015).
 - [19] J. He, S.-P. Kou, Y. Liang, and S. Feng, *Phys. Rev. B* **83**, 205116 (2011).
 - [20] J. Maciejko and A. Rüegg, *Phys. Rev. B* **88**, 241101 (2013).
 - [21] C. Hickey, P. Rath, and A. Paramekanti, *Phys. Rev. B* **91**, 134414 (2015).
 - [22] G. Jotzu, M. Messer, R. Desbuquois, M. Lebrat, T. Uehlinger, D. Greif, and T. Esslinger, *Nature* **515**, 237 (2014).
 - [23] M. Potthoff, M. Aichhorn, and C. Dahnken, *Phys. Rev. Lett.* **91**, 206402 (2003).
 - [24] J. C. Budich, R. Thomale, G. Li, M. Laubach, and S.-C. Zhang, *Phys. Rev. B* **86**, 201407 (2012).
 - [25] S. Raghu, X.-L. Qi, C. Honerkamp, and S.-C. Zhang, *Phys. Rev. Lett.* **100**, 156401 (2008).
 - [26] F. D. M. Haldane, *Phys. Rev. Lett.* **61**, 2015 (1988).
 - [27] D. Sénéchal, D. Perez, and D. Plouffe, *Phys. Rev. B* **66**, 075129 (2002).
 - [28] D. Sénéchal, *arXiv:0806.2690* (2008).
 - [29] M. Potthoff, *Eur. Phys. J. B* **32**, 429 (2003).
 - [30] G. E. Volovik, “The universe in a helium droplet.” (2003).
 - [31] Z. Wang, X.-L. Qi, and S.-C. Zhang, *Phys. Rev. Lett.* **105**, 256803 (2010).
 - [32] V. Gurarie, *Phys. Rev. B* **83**, 085426 (2011).
 - [33] Z. Wang and S.-C. Zhang, *Phys. Rev. X* **2**, 031008 (2012).
 - [34] Z. Wang and B. Yan, *Journal of Physics: Condensed Matter* **25**, 155601 (2013).
 - [35] J. Wu, J. P. L. F. Faye, D. Sénéchal, and J. Maciejko, *arXiv:1512.04498* (2015).